Power Losses in $LaFe_xCo_ySi_{1.1}$ Intermetallics near the Magnetic Phase Transition

R. Gozdur[a,*], M. Lebioda[b] and Ł. Bernacki[a]

[a]Łódź University of Technology, Department of Semiconductor and Optoelectronics Devices, B. Stefanowskiego 18/22, 90-924 Łódź, Poland

[b]Łódź University of Technology, Institute of Electrical Engineering Systems, B. Stefanowskiego 18/22, 90-924 Łódź, Poland

(Received February 2, 2015)

The paper presents magnetic parameters of $LaFe_xCo_ySi_{1.1}$ bulk specimens proving strong magnetocaloric effect. The main research work was oriented on measurements of the alloy's power losses according to IEC 60404 standards and validated with unbalanced bridge method and other methods. The measurements of the $LaFe_{10.8}Co_{1.1}Si_{1.1}$ specimens were determined in the range of temperatures near the Curie temperature where the magnetocaloric effect is the strongest. Power losses were taken into account mainly for the evaluation of usefulness and efficiency in the magnetic refrigeration applications. The results of presented measurements testify that the most suitable range of temperature and the best operational conditions are very close to the point of magnetic phase transition and slightly above it. It indicates that the magnetic state between the $T_{\Delta Smax}$ and T_c is more effective for the magnetic refrigeration applications due to lower power losses and high level of the isothermal changes of entropy. Operating temperature below the $T_{\Delta Smax}$ in ferromagnetic state is improper because of the increasing power losses which achieve the level of 130 mJ/kg for main frequency and decrease to 20 mJ/kg for the value of 0.1 Hz.

DOI: 10.12693/APhysPolA.128.98

PACS: 75.30.Sg, 75.30.Kz, 75.50.Bb

1. Introduction

The magnetocaloric effect (MCE) in paramagnetic and ferromagnetic materials is related to the isothermal changes of entropy (ΔS_m) and adiabatic changes of temperature (ΔT_{ad}) of the magnetic material under magnetizing conditions of alternating magnetic field. This magneto-thermodynamic phenomenon gives new possibilities of more efficient and green heat transfer in modern solid state cooling systems working within room-temperature (RT) magnetic refrigerators [1]. Nowadays, research works show that intermetallic compounds like As-containing alloys, La-containing alloys and Heusler alloys have the biggest potential application [2]. It has bearing on giant magnetocaloric effect mostly distinctive for intermetallics like MnAs, MnFe (As–P), Gd (Si–Ge), La–Fe–Si with magneto-structural phase transition [3–6].

Perfect MCE material should be primarily characterized by high value of entropy achieved in weak magnetic field. Good refrigerant capacity (RC) and wide range of temperatures, where strong MCE effect is available, are equally crucial. In the case of La-containing alloys those requirements are achieved near T_c in preservation of high value of RC. Cooling cycle efficiency depends on the thermal conductance of the MCE material. Thermal conductance of rare-earth-based alloys and compounds does not exceed a few W m^{-1} K^{-1}, where exemplary the $La(Fe_{0.88}Si_{0.12})_{13}$ achieves at the room temperature $k = 9$ W m^{-1} K^{-1} [7]. The La-containing alloys have attracted attention due to their low price and giant magnetocaloric effect (GMCE). The Curie temperature T_c of the $La(Fe_{0.88}Si_{0.12})_{13}$ is under room temperature, which makes them unsuitable for ambient-temperature applications. The addition of cobalt dopant is the most suitable way to enhance the Curie temperature T_c of this material. Additionally, cobalt dopant can improve the glass-forming ability (GFA) of the materials [2].

Apart from the above-mentioned dependences, electrical and magnetic properties of the MCE material play a key role. Hysteresis power losses and resistivity of the MCE material have strong influence on the efficiency of cooling cycle. The hysteresis loss is maximal near T_c and the increase of temperature, decreases hysteresis loss rapidly. This translates into the weakening of the first-order magnetic phase transition as T_c grows. Value of power losses in La-containing alloys strongly depends on the structure of material and dopants. In the case of $LaFe_{11.5}Si_{1.5}$ alloy, the energy loss is on the level of ≈20 J/kg, whereas with regard to $La_{0.7}Pr_{0.3}Fe_{11.5}Si_{1.5}$ alloy, it is more than ≈70 J/kg at 195 K [8].

Changes of entropy (ΔS_m) and total power losses display a simultaneous change thus the limitation of hysteresis power losses also reduces the MCE effect. Losses in La-containing alloys are irrelevant where changes of entropy are approximately equal to 20 J/(kg K) [8]. The value of resistivity of MCE material has an impact on eddy currents. Forms of MCE materials such as thin sheets, micro-wires or pellets allow to increase resistivity and significantly limits eddy currents [9].

*corresponding author; e-mail: roman.gozdur@p.lodz.pl

The design of the solid state refrigerators which work effectively in wide range of temperature needs MCE materials with very high ΔS_{m}. Pursued research work indicates the particular difficulty of elaboration of intermetallic compounds which meet above-mentioned terms. The composite of the component parts with different T_{c} is indirect method of stretching the temperature range and shaping the profile of the ΔS_{m} distribution. A limitation of the method is the rise of power losses in inactive parts which are in the ends of the considered range of operating temperature. The components with the highest T_{c} play a crucial role. These components are in ferromagnetic state almost ever, thus it has influence on the magnetic field distribution and generation of the power losses related to magnetization process.

The paper refers to the research work with bulk specimens made of $\mathrm{LaFe}_x\mathrm{Co}_y\mathrm{Si}_{1.1}$. Performed tests involve magnetic hysteresis losses in the range of magnetic saturation where the magnetic polarization density specimen achieves the highest, possible value. Estimation of the losses significant owing to the limitation or elimination is virtually impossible.

2. MCE samples, instrumentation and experimental procedure

The application of laboratory magnetometers like the Lakeshore VSM/PCM/AGM or the Quantum Design PPMS/MPMS is not possible owing to the large dimensions of the tested core. In this case all tests and measurements of MCE specimens can be performed in thermostatic chamber with standard methods [10]. Measurements achieved in this way are more reliable and can be carried out with the application of typical measurement systems like Brockhaus, Magnet-Physic and other systems based on recommendations of IEC60404-4, IEC60404-6 standards.

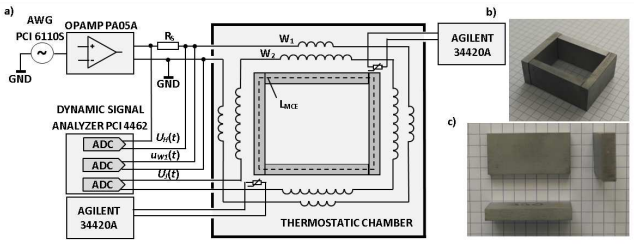

Fig. 1. (a) Measurement diagram and $\mathrm{LaFe}_{10.8}\mathrm{Co}_{1.1}\mathrm{Si}_{1.1}$, (b) arrangement of the four specimens in the tested core, (c) the specimen of the $\mathrm{LaFe}_{10.8}\mathrm{Co}_{1.1}\mathrm{Si}_{1.1}$.

The tested MCE core was assembled with the same four specimens (Fig. 1c) of $\mathrm{LaFe}_{10.8}\mathrm{Co}_{1.1}\mathrm{Si}_{1.1}$ which do not tend axial magnetic anisotropy. The specimens $36 \times 18 \times 5$ mm without coating were applied for the tests in the arrangement presented in Fig. 1b. Total mass m_{MCE} of the core amount to $m_{\mathrm{MCE}} = 0.094$ kg and the value of the density of the sintered compound was equal to $\rho = 7288\ \mathrm{kg/m^3}$. The average magnetic path L_{MCE} of the core has been calculated from overall dimensions of the core and for further analysis the value of $L_{\mathrm{MCE}} = 0.149$ m was assumed. The surface quality and high-dimensional accuracy below 0.1 mm reduce magnetic reluctance of the gaps between components significantly. Therefore, it can be assumed that the core creates closed magnetic path.

Each component of the core was equipped with section of pickup coil and exciting coil. The coils were made as single layer windings and connected in series as 4×22 and 4×51 turns, respectively.

Assembled core was locally glued and closed in thermostatic chamber with thermoelectric module MCHPE-128-10-05-E. Available range of temperature inside the chamber from 280 K to 345 K could be controlled with 0.1 K accuracy. The settling time of required temperature in the chamber averaged out at 1000 s every time. Two temperature sensors were mounted on the opposite sides of the core. Measurements of the temperature were done with the application of 4-wire, thin-film PT100 class A resistors (Mfr IST) and Keysight 34420A multimeters.

Measurements of power losses and hysteresis loops were carried out with the author's system (Fig. 1a) which meets requirements of the above-mentioned standards. The system has been calibrated by measurement of the certified magnetic specimens from The Physikalisch-Technische Bundesanstalt (PTB) metrology institute. Additionally, the measurements were compared and validated with results obtained from hysteresis loops, standard wattmeter method, and unbalance bridge method (UBM) presented in the papers [11, 12]. Measurements of magnetic strength field $H(t)$ were carried out with indirect method as measurements of the voltage drop $u_H(t)$ across the shunt resistor R_{S}. Instantaneous values of the field $H(t)$ were calculated according to Eq. (1):

$$H\left(t\right) = \frac{w_1}{R_{\mathrm{S}} L_{\mathrm{Fe}}} u_H\left(t\right), \tag{1}$$

where w_1 — number of turns of exciting coil, R_{S} – shunt resistance [Ω], L_{MCE} — average magnetic path [m], $u_H(t)$ — voltage drop across the resistor R_{S} [V].

The relation between the magnetic polarization $J(t)$ and voltage $u_J(t)$ induced in the pickup coil w_2 is expressed as (2):

$$J\left(t\right) = B\left(t\right) - \mu_0 H\left(t\right) = w_2^{-1} S_{\mathrm{MCE}}^{-1} \int_0^T u_J\left(t\right) \mathrm{d}t - \frac{w_1}{R_{\mathrm{S}} L_{\mathrm{MCE}}} \mu_0 u_H\left(t\right), \tag{2}$$

where u_J(t) — voltage of the pickup coil w_2 [V], w_2 — number of turns of the coil w_2, μ_0 — magnetic constant [H/m], S_{MCE} — cross-section of the core [$\mathrm{m^2}$].

After putting together formulae (1) and (2) into general equation for power loss one achieves relation (3) which defines normalized total power loss:

$$P_{\mathrm{S}} = \frac{f}{\rho} \oint H \,\mathrm{d}(B - \mu_0 H) = \frac{f}{\rho} \oint H \,\mathrm{d}J, \tag{3}$$

where P_{S} — total power loss [W/kg], f — frequency of the magnetization process [Hz], ρ — volumetric density [kg/m^3].

Sinusoidal shape of the magnetizing current which supplies the exciting coil w_2 was hold through the shaping of the voltage $u_H(t)$ and controlling the value of the form factor FF. The arbitrary wave-form generator with 16-bits DA converter NI PCI1610 and precision power amplifier Apex PA05A create together the power supply stage. Wave forms of the acquired voltages $u_H(t)$, $u_J(t)$, $u_{w1}(t)$ used for calculation of the $H(t)$, $J(t)$, $J(H)$, $P_{\mathrm{S}}(t)$ were sampled with the maintained the condition $f_{\mathrm{sampling}}/f = 4000$. The dynamic signal analyser NI PCI-4462 with four 24-bits AD converters was used for the acquisition of all wave forms.

Step-by-step measurement procedure of the power losses was performed every time as the following sequence: demagnetization of the tested core, shaping of the magnetizing current wave form, setting and stabilization of the temperature inside the chamber, the measurement of the power losses and hysteresis loops according to standard method and UBM method. The budget of uncertainty for the measurements of power loss were estimated. Taking into account the budget, the calculated relative uncertainty never exceed 5% of measured value.

3. Measurement results and discussion

Main research work concerns the measurements and the analysis of the power losses related to the magnetization process. The mentioned losses have a disadvantageous influence on magneto-thermodynamic energy balance. The analysis of the relation between the losses and temperature round the magnetic phase transition allows to determine optimum range of operational temperatures where magnetocaloric effect inducing heat exchange is the most efficient. The approach to the power losses generated in the MCE materials can be similar to that in the other ferromagnetic materials. Total power losses are separated as steady-state hysteresis loss P_H component and dynamic losses component. Classical, eddy current loss P_{CL} and excess loss P_{EX} components constitute the dynamic losses and depend on the frequency [13, 14]. All the above-mentioned losses cumulate themselves $P_{\mathrm{S}} = (P_H + P_{\mathrm{CL}} + P_{\mathrm{EX}})$ and lead to the self-heating MCE material during the magnetization. Whereas hysteresis loss component is permanent, the dynamic component of the losses highly depends on the frequency according to the power law which is shown in Figs. 2 and 3. The rise of the losses is primarily the outgrowth of the eddy currents. Therefore, the measurements were carried out in the range of low frequencies from 0.01 Hz to 50 Hz which involves potential applications of MCE materials in active magnetic regenerators (AMR) [15].

In the applications, the time constant of the heat processes limits the frequency of magneto-thermodynamic

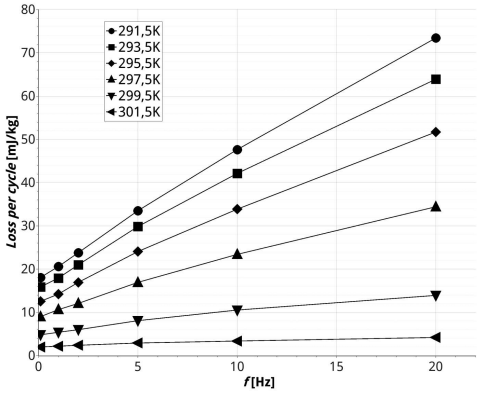

Fig. 2. Total power losses per cycle from quasi-static cut-off frequency to 20 Hz at given temperature 291.5 K and constant peak magnetic flux density 0.78 T.

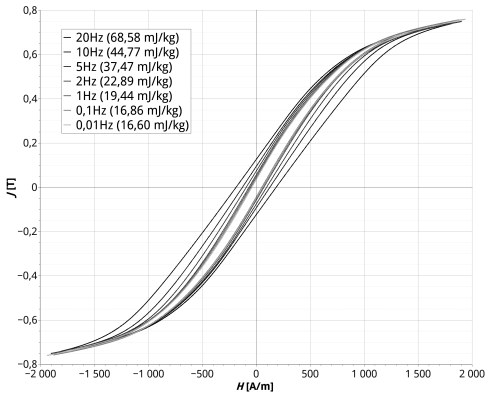

Fig. 3. Hysteresis loops from quasi-static cut-off frequency to 20 Hz at given temperature 291.5 K and constant peak magnetic flux density 0.78 T.

cycle. Nowadays, frequency of the cycle does not exceed 2.0 Hz and determines the tested range of frequency 0.1–20 Hz [15]. It leads to the lower level of power losses but also decreases the cooling efficiency as the result of reduced number of thermodynamic cycles.

The magnetic phase transition order-disorder of the tested $\mathrm{LaFe}_x\mathrm{Co}_y\mathrm{Si}_{1.1}$ alloy in the composition $\mathrm{LaFe}_{10.8}\mathrm{Co}_{1.1}\mathrm{Si}_{1.1}$ is achieved in temperature of $T_{\mathrm{c}} = 300.0$ K, whereas maximal changes of entropy being an indication of the magnetocaloric effect are followed by temperature of $T_{\Delta \mathrm{Smax}} = 295.5$ K. Temperature range of the ferromagnetic-paramagnetic transition is varied from cobalt dopant and value of magnetic flux density. The considered composition has approximately 10 K range. Taking into account the magnetization process in the temperature range 290.5 K $< T <$ 305.5 K it is worth noting that the highest efficiency of the alloy peaks in the transition point (Fig. 4). The energy loss per cycle expressed through the area of the hysteresis loops (Fig. 5) is acceptable in this range as well. Magnetization process in the descending temperature below T_{c} leads to the considerable rise of the total losses (Fig. 4, Fig. 5) however, it improves the entropy.

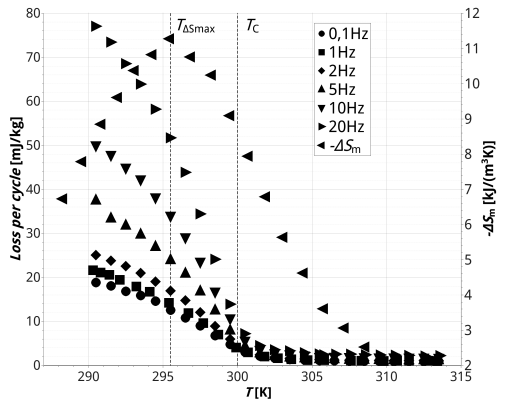

Fig. 4. Total power losses per cycle near the magnetic phase transition (290 K–305 K).

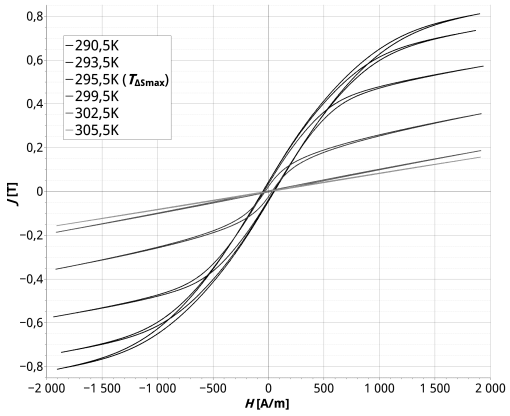

Fig. 5. Magnetic hysteresis loops near the magnetic phase transition (290 K–305 K).

Further decrease of temperature below $T_{\Delta \mathrm{Smax}}$ multiplies losses and flip trends of the entropy. The analysis of the measurements testifies that the setting of $LaFe_xCo_ySi_{1.1}$ operating point in the deep ferromagnetic state is highly adverse. It concerns all frequencies even the range of ultra-low frequencies where hysteresis loss component is prevailing. The limitation of the hysteresis losses is possible by the changes of structure and stoichiometry of the alloy but simultaneously it reduces MCE. The rise of total losses in ferromagnetic state may limit the efficiency of hybrid AMRs. Only assembling of MCE components or mixing of alloys with different T_c currently allow to gain operational range of temperature [5, 6, 16, 17]. Obtained results point out that decreasing temperature of AMR rises power losses related to magnetization process. When current temperature of hybrid AMR is far below T_c of certain MCE components then these components will only be a source of heat for AMR.

4. The evaluation of power losses

The correct determination of the hysteresis loss component and separation of total power losses require in practice definition of cut-off frequency of the magnetization. The magnetization process below the cut-off frequency may be acknowledged as quasi-static and total power losses are identified with hysteresis loss [14].

The cut-off frequency of the $LaFe_xCo_ySi_{1.1}$ core occurs in range below 1 Hz. The measurement's results (Fig. 6) indicate that the further descending of magnetizing frequency below 0.1 Hz does not change the process. The value of total power losses and the shape of hysteresis loops are not different from the value of the scatter caused by the uncertainty of the measurements.

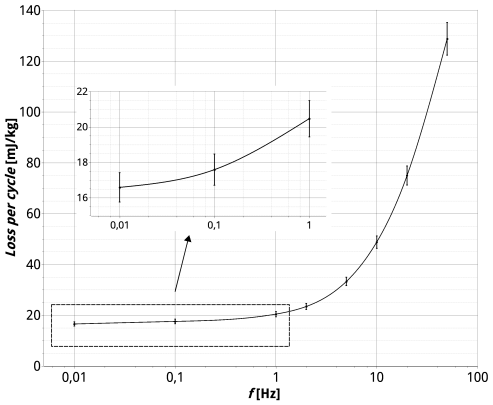

Fig. 6. Quasi-static cut-off frequency determination with uncertainty criterion.

Estimated relative uncertainty of the power losses measurement on the level of 5% determines the value of $f_{\mathrm{cut-off}} = 0.1$ Hz when the course of the magnetization process is quasi-static.

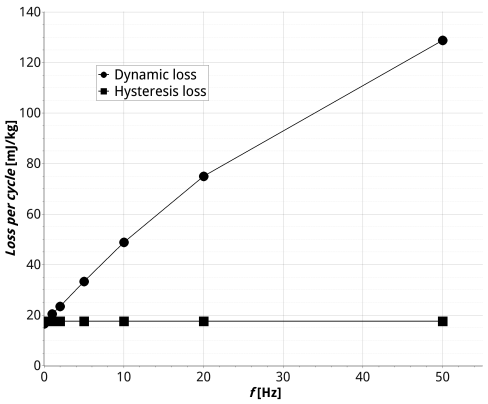

Fig. 7. Total losses of $LaFe_{10.8}Co_{1.1}Si_{1.1}$ with hysteresis loss and dynamic loss components (classical and excess losses).

On the basis of the cut-off frequency $f_{\mathrm{cut-off}}$ the separation of the total losses into hysteresis and dynamic components was carried out (Fig. 7). The power losses of the core made of $LaFe_{10.8}Co_{1.1}Si_{1.1}$ show similar changes below T_c and $T_{\Delta \mathrm{Sm}}$ like common FeSi grain oriented lamination. Therefore well-known approaches to the detailed analysis of losses may be applied [10, 13, 18].

The value of hysteresis power loss can be evaluated with the use of known, empirical equation like Steinmetz, Richter, Anderson et al. [18, 19]. General Steinmetz equation (SE) has still been evolving due to a small number of required parameters [20–23]. Prediction of the hysteresis loss P_{sS} can be simply made from Eq. (4) if the value of Steinmetz coefficient k_S and exponent α in SE are known. The Steinmetz coefficient k_S is also empirically evaluated according to the relation (5) using measurement data of H_c and J_m from hysteresis loops (Fig. 3, Fig. 5) [20].

$$P_{sS} = k_S f J_m^{\alpha}, \tag{4}$$

$$k_S = \frac{\pi \cdot H_c}{\rho \cdot J_m}, \tag{5}$$

where P_{sS} — hysteresis loss evaluated from SE [W/kg], k_S — Steinmetz coefficient determined in $T = 291.5$ K [W/(kg Hz T^{α})], f — frequency of the magnetization process [Hz], J_m — maximal density of magnetic polarisation [T], α — exponent of the SE, H_c — magnetic coercive force [A/m], ρ — volumetric density of $LaFe_{10.8}Co_{1.1}Si_{1.1}$ alloy [kg/m^3].

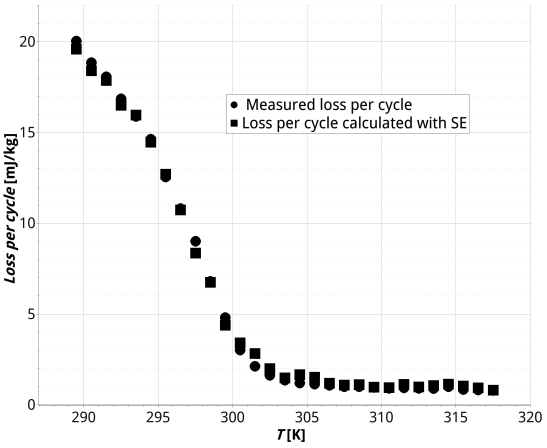

Fig. 8. Comparison of hysteresis loss component measured and estimated with SE.

The Steinmetz equation was applied for the evaluation of hysteresis loss in the $LaFe_{10.8}Co_{1.1}Si_{1.1}$ in the temperature range near magnetic phase transition. The values of SE coefficient and the exponent were determined in the temperature of $T = 291.5$ K. Subsequently, hysteresis losses were calculated from Eq. (6) in considered range of temperature and compared with the measurement data (Fig. 8).

$$\frac{P_{sS}}{f} = 0.031 J_m^{2.011}, \quad k_s \approx 0.031, \quad \alpha = 2.011. \tag{6}$$

The consistence of predicted and measured data is attained in both ferromagnetic and paramagnetic states near the magnetic phase transition. Therefore, the simple Steinmetz formula might be applied to the evaluation hysteresis losses in wide range of magnetic flux density and different compositions of $LaFe_xCo_ySi_{1.1}$ alloy.

The discussed prediction method was used in the quasi-paramagnetic state slightly above T_c (Fig. 9) although the Steinmetz equation is preferably used for the estimation hysteresis losses in the materials with pure and stable ferromagnetic state. Empirical formula (5) defines the correlation of the coefficient k_S with J_m and H_c. Both magnetic properties drop above T_c and it leads to the randomly scattered values of the coefficient k_S above T_c (Fig. 9). The deviation of the k_S around the average value of 0.0531 is closely connected with fluctuations of very small values of the coercive force H_c and magnetic polarization J_m presented in Fig. 10. The prediction error fractionally raises in the temperature range above Curie temperature, but still it conforms with the experimental data.

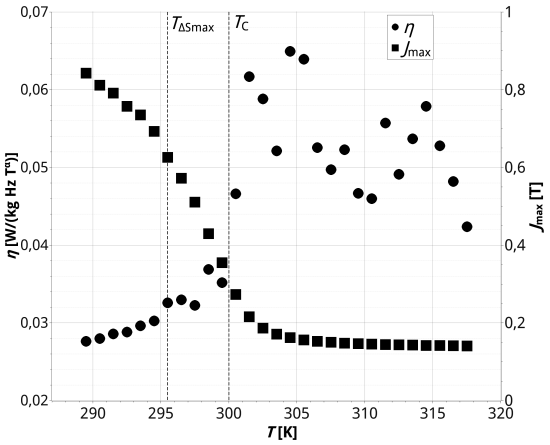

Fig. 9. Fluctuations of the Steinmetz coefficients k_S around T_c.

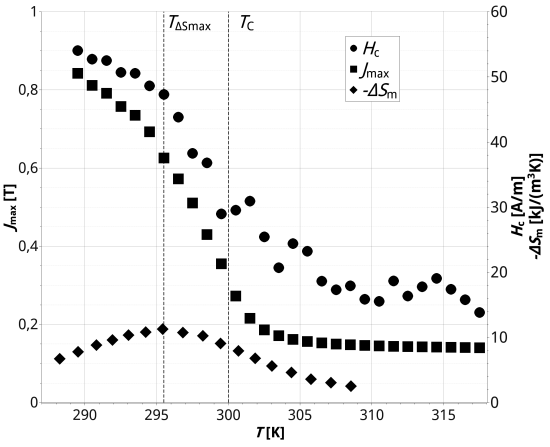

Fig. 10. Changes of the magnetic properties H_c, J_m determined from the hysteresis loops.

In the temperature range below the $T_c = 294.6$ K the value of the estimated Steinmetz coefficient k_S varies slightly and it can be assumed as $k_S = 0.031$ over the temperature range which was taken into account in the research. The determined value of α exponent on the level $\alpha = 2.011$ has been validated for the assumed k_S as well.

5. Conclusions

The obtained measurement's results confirm a typical strong influence of the temperature on power losses in $LaFe_xCo_ySi_{1.1}$ materials. Magnetic phase transition determines the magnetization process and decreases value of power losses. The magnetic state between the $T_{\Delta Smax}$ and T_c is more effective for the magnetic refrigeration applications due to lower power losses and high level of the isothermal changes of entropy. Operating temperature below the $T_{\Delta Smax}$ in ferromagnetic state is highly adverse.

Acknowledgments

The work was carried out with financial support from Polish National Science Centre under the grant agreement No. 6370/B/T02/2011/40.

References

[1] M. Tishin, Y.I. Spichkin, *The Magnetocaloric Effect and Its Applications*, Institute of Physics Publishing, London 2003.

[2] H.Y. Nguyen, T.T. Pham, H.D. Nguyen, D.T. Tran, T. Phan, Ch.Y. Seong, H.D. Nguyen, *Adv. Natural Sci. Nanosci. Nanotechnol.* **2**, 4 (2013).

[3] J. Łażewski, P. Piekarz, J. Toboła, B. Wiendlocha, P.T. Jochym, M. Sternik, K. Parlinski, *Phys. Rev. Lett.* **104**, 147205 (2010).

[4] L. Mañosa, A. Planes, M. Acet, *J. Mater. Chem. A* **16**, 4925 (2013).

[5] P. Gębara, P. Pawlik, I. Škorvánek, J. Bednarcik, J. Marcin, Š. Michalik, J. Donges, J.J. Wysłocki, B. Michalski, *J. Magn. Magn. Mater.* **372**, 201 (2014).

[6] P. Gębara, P. Pawlik, I. Škorvánek, J. Marcin, J.J. Wysłocki, *Acta Phys. Pol. A* **118**, 910 (2010).

[7] J.A. Turcaud, K. Morrison, A. Berenov, N.McN. Alford, K.G. Sandeman, L.F. Cohen, *Scr. Mater.* **68**, 510 (2013).

[8] J. Shen, B. Gao, H.W. Zhang, F.X. Hu, Y.X. Li, J.R. Sun, B.G. Shen, *Adv. Mater.* **21**, 4545 (2009).

[9] A. Biswas, Y.Y. Yu, N.S. Bingham, H. Wang, F.X. Qin, J.F. Sun, S.C. Yu, V. Franco, H. Srikanth, M.H. Phan, *J. Appl. Phys.* **115**, 17A318 (2014).

[10] F. Fiorillo, *Characterization and Measurement of Magnetic Materials*, Elsevier 2004.

[11] R. Gozdur, A. Majocha, *Przegląd Elektrotechniczny* **4**, 79 (2010) (in Polish).

[12] R. Gozdur, A. Majocha, *Electr. Machin. — Trans. J.* **100**, 175 (2013).

[13] G. Bertotti, *IEEE Trans. Magn.* **24**, 621 (1988).

[14] F. Fiorillo, *J. Magn. Magn. Mater.* **242–245**, 77 (2002).

[15] P. Bansal, E. Vineyard, O. Abdelaziz, *Int. J. Sust. Built Env.* **1**, 85 (2012).

[16] P. Gębara, P. Pawlik, I. Škorvánek, J. Marcin, K. Pawlik, A. Przybył, J.J. Wysocki, M. Szwaja, K. Filipecka, *Acta Phys. Pol. A* **126**, 166 (2014).

[17] P. Gębara, P. Pawlik, E. Kulej, J.J. Wysłocki, K. Pawlik, A. Przybył, *Opt. Appl.* **39**, 761 (2009).

[18] J. Turowski, M. Turowski, *Engineering Electrodynamics: Electric Machine, Transformer, and Power Equipment Design*, CRC Press 2014.

[19] S. Kobayashi, N. Kikuchi, S. Takahashi, H. Kikuchi, Y. Kamada, *J. Magn. Magn. Mater.* **322**, 1515 (2010).

[20] M. Popescu, D.M. Ionel, A. Boglietti, A. Cavagnino, C. Cossar, M.I. McGilp, *IEEE Trans. Ind. Appl.* **46**, 1389 (2010).

[21] L. Svensson, K. Frogner, P. Jeppsson, T. Cedell, M. Andersson, *J. Magn. Magn. Mater.* **324**, 2717 (2012).

[22] W.J. Yuan, J.G. Li, Q. Shen, L.M. Zhang, *J. Magn. Magn. Mater.* **320**, 76 (2008).

[23] D. Aguglia, M. Neuhaus, *Power Electron. Appl.* EPE2013, 2013, p. 1.